Optimal molecular crowding accelerates group II intron folding and maximizes catalysis

Bishnu P. Paudel[a,b,1], Erica Fiorini[c,1], Richard Börner[c,1], Roland K. O. Sigel[c,2], and David S. Rueda[a,b,2]

[a]Molecular Virology, Department of Medicine, Imperial College London, London W12 0NN, United Kingdom; [b]Single Molecule Imaging, Medical Research Council London Institute of Medical Sciences, London W12 0NN, United Kingdom; and [c]Department of Chemistry, University of Zurich, 8057 Zurich, Switzerland

Edited by Joseph D. Puglisi, Stanford University School of Medicine, Stanford, CA, and approved October 5, 2018 (received for review May 21, 2018)

Unlike in vivo conditions, group II intron ribozymes are known to require high magnesium(II) concentrations ([Mg^{2+}]) and high temperatures (42 °C) for folding and catalysis in vitro. A possible explanation for this difference is the highly crowded cellular environment, which can be mimicked in vitro by macromolecular crowding agents. Here, we combined bulk activity assays and single-molecule Förster Resonance Energy Transfer (smFRET) to study the influence of polyethylene glycol (PEG) on catalysis and folding of the ribozyme. Our activity studies reveal that PEG reduces the required [Mg^{2+}], and we found an "optimum" [PEG] that yields maximum activity. smFRET experiments show that the most compact state population, the putative active state, increases with increasing [PEG]. Dynamic transitions between folded states also increase. Therefore, this study shows that optimal molecular crowding concentrations help the ribozyme not only to reach the native fold but also to increase its in vitro activity to approach that in physiological conditions.

molecular crowding | large-ribozyme folding | single-molecule FRET | group II intron ribozyme | excluded volume effect

Cells are compact and crowded due to the presence of high concentrations of macromolecules such as nucleic acids, proteins, metabolites, and organelles that can occupy up to one-third of the total volume (1–7). Crowded environments not only limit the free diffusion of all biomolecules but also lead to spatial confinement that originates from steric hindrance, usually referred to as excluded volume effect (3, 5, 8). All cellular processes, including enzymatic reactions as well as nucleic acid and protein folding and their interactions, have evolved under such conditions, which are very different from in vitro dilute solutions.

RNA molecules fold into specific 3D structures to become functional (9). Cofactors, such as metal ions, play a key role in RNA folding by screening the negative charges of the phosphate backbone and mediating tertiary contact formation (10–12). In crowded environments, RNA folding and catalysis can be affected by excluded volume effects, changes in diffusion rate constants, viscosity, or the dielectric constant (3, 13–17). Numerous protein folding studies have shown that excluded volume effects can accelerate native (N)-state formation (18–24). Similarly, crowding agents have been shown to affect nucleic acid folding, such as DNA G-quadruplexes (25) and ribozymes (13–15, 17, 26–29).

In the case of small and medium-size ribozymes, molecular crowding accelerates folding and decreases metal-ion requirements (13, 15, 30). However, it remains unclear how crowding agents affect large-ribozyme folding and catalysis. To address this, we use the D135 ribozyme, a well-characterized model system derived from the ai5γ group IIB intron of *Saccharomyces cerevisiae* mitochondria (31–34). Group II intron ribozymes self-splice from pre-mRNA through two transesterification reactions (35–37). Consisting of six structural domains (D1 to D6), group II introns include a conserved catalytic core that resembles the nuclear spliceosome (37–40). D135 is a minimal ribozyme that efficiently catalyzes the hydrolytic cleavage of the 5′ splice site (Fig. 1*A*) (35, 36). Studies in vitro have shown that D135 adopts the N state through at least two distinct conformations: an extended intermediate (I) state and a folded intermediate state (31, 32, 41). The low-populated N state is stabilized by substrate binding or the presence of the Mss116 helicase (31, 34).

Here, we combine bulk cleavage assays and single-molecule folding studies to characterize the D135 ribozyme folding and catalytic 5′-exon hydrolytic cleavage in the presence of crowding agents. Similar to small ribozymes, increasing crowding accelerates folding and decreases Mg^{2+} requirements. In contrast, our data show that above an "optimal" molecular weight and weight per volume fraction (wt/vol) of the crowding agent, the ribozyme's activity decreases again. These observations raise the interesting possibility that, for large ribozymes, maximum activity is reached at an optimal cavity size.

Results

Macromolecular Crowding Reduces Mg^{2+} Requirement for Catalysis. To study the influence of macromolecular crowding on the activity of large ribozymes, we use the D135-L14 construct, previously designed for single-molecule Förster Resonance Energy Transfer (smFRET) measurements (Fig. 1*A*), in which DNA oligonucleotides carrying the donor or acceptor fluorophore hybridize to artificial loops in D1 and D4 (31, 32, 34). In the absence of crowding agents, we confirm that our labeling strategy

Significance

Biological processes take place in living cells and have adapted to environmental conditions such as temperature, salt concentration, and high-density cellular contents. However, our molecular understanding of most biological processes relies on in vitro experiments under nonphysiological, highly diluted, and high-salt conditions. To overcome this, we mimic the cellular environment by introducing crowding agents. To understand how such conditions affect large-ribozyme folding and function, we studied a group IIB intron ribozyme under crowded, low-salt conditions. The data show how crowded environments enhance the activity of such large ribozymes, even in low-salt concentrations. Interestingly, we find that "optimal" crowding yields maximum activity, beyond which dense crowding becomes detrimental for activity.

Author contributions: B.P.P., E.F., R.B., R.K.O.S., and D.S.R. designed research; B.P.P., E.F., and R.B. performed research; B.P.P., E.F., R.B., R.K.O.S., and D.S.R. analyzed data; and B.P.P., E.F., R.B., R.K.O.S., and D.S.R. wrote the paper.

The authors declare no conflict of interest.

This article is a PNAS Direct Submission.

[1]B.P.P., E.F., and R.B. contributed equally to this work.

[2]To whom correspondence may be addressed. Email: roland.sigel@chem.uzh.ch or david.rueda@imperial.ac.uk.

This article contains supporting information online at www.pnas.org/lookup/suppl/doi:10.1073/pnas.1806685115/-/DCSupplemental.

Published online November 5, 2018.

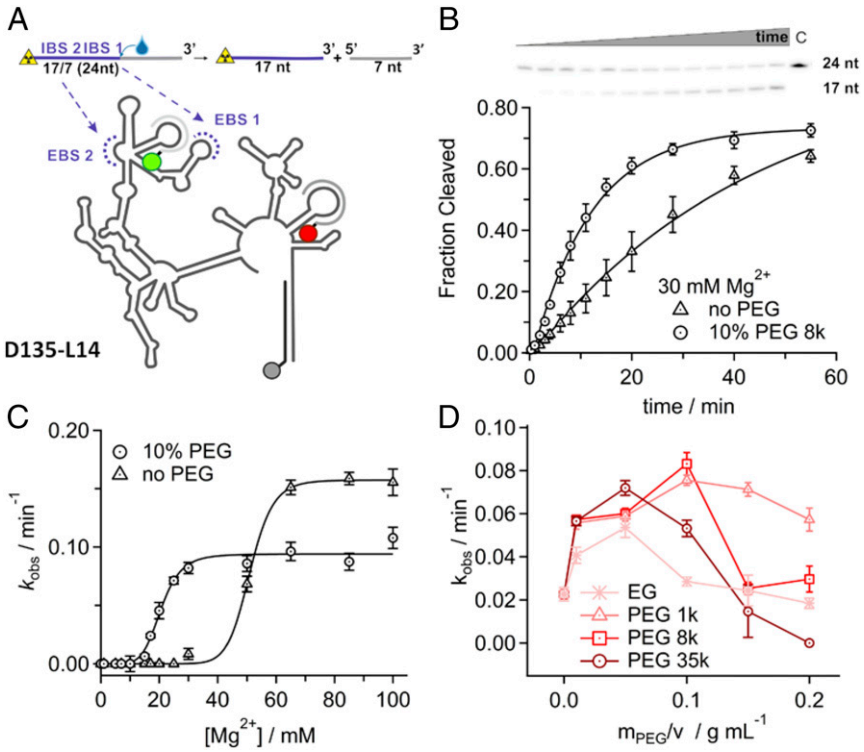

Fig. 1. Influence of a crowded environment on ribozyme catalysis. (*A*) Scheme of the radioactive activity assay: The cleavage reaction catalyzed by the ribozyme D135-L14 was followed and quantified using radioactively ^{32}P-5′-end-labeled substrate 17/7, PAGE analysis, and subsequent phosphoimaging. EBS, exon binding site; IBS, intron binding site. (*B*) Effect of 10% PEG 8000 on the cleavage activity at 30 mM Mg^{2+}. (*C*) Rate constants determined via the cleavage assay at different [Mg^{2+}] in the absence and presence of 10% PEG 8000. (*D*) PEG screening for optimal crowding conditions. Rate constant k_{obs} depends on the PEG wt/vol (0.1 g mL^{-1} ≡ 10%) and the PEG molecular weight (PEG 1000, 8000, or 35000) at 30 mM Mg^{2+}. Activity optimum is at a wt/vol of ∼10% PEG 8000. All error bars (SD) from triplicate experiments.

does not affect cleavage of the 17/7 substrate under single-turnover conditions (Fig. 1 *A* and *B* and *SI Appendix*, Table S1) (31, 42). In the presence of 10% PEG 8000, we observed an approximtely fourfold increase in cleavage rate constant (Fig. 1*B*). To confirm that this is a specific macromolecular crowding effect, we measured cleavage activity in the presence of ethylene glycol (EG), the PEG monomer, which does not yield the same effect (*SI Appendix*, Fig. S1). Although EG and PEG have significant structural differences, EG is a suitable monomeric control compound because it shares functional moieties such as hydroxyl groups and hydrogen bonding lone pairs on the ether oxygens (13). Varying the mixing order of the substrate, ribozyme, and crowding agent does not affect the cleavage rate constants (*SI Appendix*, Figs. S1 and S2). These results show that under these conditions, macromolecular crowding increases the cleavage activity.

To test whether macromolecular crowding decreases the Mg^{2+} requirement for D135-L14 catalysis, we measured the ribozyme's activity in the absence and presence of 10% PEG 8000. In the absence of PEG, the activity increases cooperatively with increasing [Mg^{2+}] (Fig. 1*C*). A fit to the Hill equation yields K_{Mg2+} = 51 ± 2 mM, with very low activity below 20 mM Mg^{2+}, in agreement with previous results (31, 33). In the presence of 10% PEG 8000, the titration midpoint shifts to lower [Mg^{2+}] (K_{Mg2+} = 20 ± 1 mM; Fig. 1*C*). Interestingly, the ribozyme reaches maximum activity at ∼30 mM Mg^{2+}. However, at [Mg^{2+}] ≥60 mM, the ribozyme is ∼1.5-fold faster in the absence of PEG. This difference could be caused by a viscosity-induced decrease in diffusion in the presence of PEG. A viscosity-corrected rate constant estimation (26, 43) shows that the ribozyme's activity is approximately fourfold higher in the presence of PEG (10%) (*SI Appendix*, Fig. S2*B*). In summary, these results show that the presence of macromolecular crowders increases the ribozyme's activity and lowers the Mg^{2+} requirement.

Intermediate Crowding Yields the Ribozyme's Optimal Activity. To determine the volume exclusion effect, we measured the ribozyme's cleavage activity at increasing PEG wt/vol at 30 mM Mg^{2+}, which yields the most significant difference between the absence and presence of PEG (Fig. 1*C*). As expected, increasing the PEG wt/vol from 0 to 10% results in a systematic increase in the observed cleavage rate constant (Fig. 1*D*). Surprisingly, increasing the PEG wt/vol above 10% results in a decrease in the ribozyme's activity. A possible explanation for this observation is that above a critical PEG concentration, the average cavity size no longer fits the hydrodynamic radius of the ribozyme, thereby hindering either ribozyme folding or catalysis. To test this, we repeated the titration with PEG of larger and smaller molecular weights (Fig. 1*D*). The smaller PEG (PEG 1000) shifted the maximum ribozyme activity to 10–15% wt/vol, whereas the larger PEG (PEG 35000) shifted the maximum ribozyme activity to 5% wt/vol. These results are in agreement with the idea of an optimal cavity size for large-ribozyme folding and catalysis.

Molecular Crowding Favors the Ribozyme's Most Compact State. To distinguish between crowding effects on folding and catalysis, we use smFRET to measure the influence of molecular crowded environments on the ribozyme's folding. To visualize single D135-L14 ribozymes, we hybridized three DNA oligonucleotides, two carrying the FRET pair Cy3 and Cy5 and a third one carrying biotin to immobilize the ribozyme onto the microscopic quartz slide (Fig. 1*A*) (31). Prior smFRET studies have shown that the ribozyme adopts at least three FRET states in the

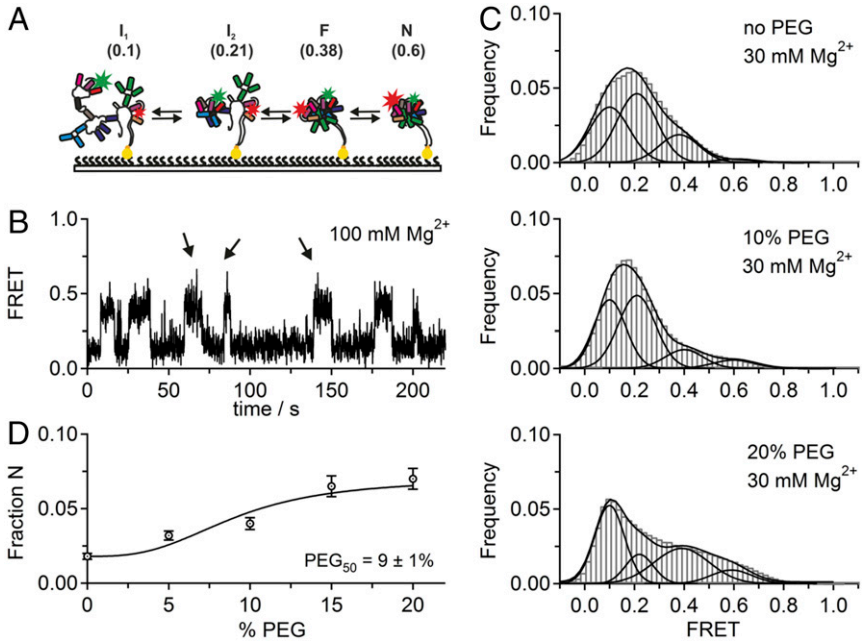

Fig. 2. Influence of a macromolecular crowded environment on ribozyme folding. (*A*) Folding pathway of the D135-L14 ribozyme. Folding states determined via smFRET. F, folded intermediate. (*B*) A FRET trajectory at high [Mg^{2+}]. The transiently occurring, most compact state (N) is indicated by arrows. (*C*) Effect of different PEG 8000 concentrations at 30 mM (low) Mg^{2+}. (*D*) Fraction of state N (circle) depending on the PEG concentration. Error bars (SD) are determined from Gaussian fits.

presence of high [Mg^{2+}] (31, 32). A low FRET state (~0.1) was attributed to be either a donor-only species or the unfolded state in the absence of Mg^{2+}. smFRET RNA–protein binding assays of the helicase Mss116 binding to the ribozyme showed a shift of the low, ~0.1 FRET state to higher values (~0.2) when the helicase was present (34). Here, with a probe laser for alternate laser excitation (44) and improved signal-to-noise ratio, we found that the I state in the low FRET region splits into two states that interconvert within single FRET time trajectories (Fig. 2*B* and *SI Appendix*, Fig. S4*A*). We name these I_1 (~0.1 FRET) and precompact folded intermediate (I_2, ~0.21 FRET). The folding pathway remains consistent with our previous results, with at least four distinct conformational states, including an additional on-path intermediate (Fig. 2*A*); the most compact state is only transiently present, as indicated by arrows in the example FRET trace (Fig. 2*B*). The same FRET states are also observed in the presence of PEG.

Only a small fraction of the most compact state (N) is present (≤2%) under standard buffer conditions and with 30 mM Mg^{2+} (Fig. 2*C*). However, the fraction of the most compact state gradually increases by increasing the PEG percentages and finally saturates above 10%. We obtain a midpoint $PEG_{50} = 9 \pm 1\%$ for ribozyme folding by fitting the fraction of the N state as a function of crowding agent concentration to a binding model (*SI Appendix*, *SI Methods*), indicating that molecular crowding favors and increases the formation of the most compact state, N (Fig. 2*D*).

Thirumalai and coworkers (45) have previously shown, using all-atom molecular dynamics simulations and coarse-grained modeling of a small 22-nt RNA hairpin, that cosolutes that interact favorably with multiple bases simultaneously can stabilize the hairpin more than a noninteracting crowding agent of the same size. To rule out that the observed effect is not due to specific interactions between the group II intron and PEG, we conducted a series of control experiments in the presence of EG and dextran (molecular weight of 10,000). Akin to PEG, we observed that the stability of the group II intron increases in dextran, but not in the presence of EG (*SI Appendix*, Fig. S3). This indicates that the observed effect is not caused by specific interactions between PEG and the ribozyme.

Molecular Crowding Agents Reduce Mg^{2+} Requirement to Fold into the Most Compact State. Group II intron folding studies have traditionally been carried out in high ionic strength buffers (i.e., 500 mM KCl and high amounts of $MgCl_2$) that are far from the physiological range (e.g., intracellular/mitochondrial concentrations of ~1 mM Mg^{2+} and ~150 mM K^+) (31, 34, 46). To show how crowding agents affect the requirement of divalent metal ions for folding, we carried out experiments at different [Mg^{2+}] in the presence and absence of crowding agents (Fig. 3*A*). In particular, we performed a Mg^{2+} titration in the presence of 10%

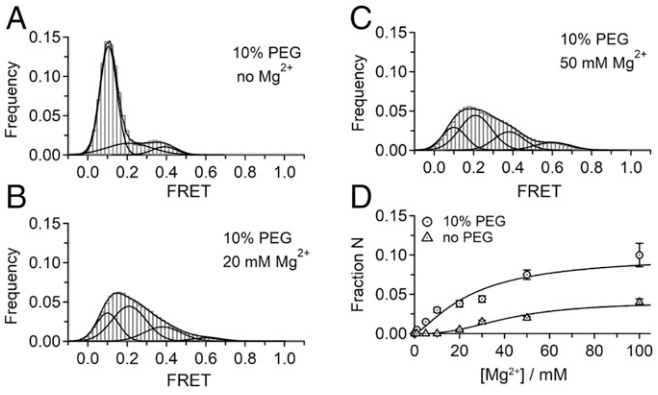

Fig. 3. Influence of a macromolecular crowded environment on the Mg^{2+} requirement for ribozyme folding. (*A–C*) Effect of 10% PEG 8000 at different [Mg^{2+}]. (*D*) Fraction of the most compact state (N) as a function of [Mg^{2+}] with (circle) and without (triangle) 10% PEG 8000. Error bars (SD) from Gaussians fits.

PEG 8000 (i.e., the optimal conditions determined from our cleavage assays) (Fig. 1).

In the absence of Mg^{2+}, we observed only three FRET states, with the low (0.1) FRET state being the most populated (Fig. 3*A*). This state corresponds to the I_1 state. Under these conditions, the most compact state, N, is not observed, confirming that Mg^{2+} ions are required for N-state formation, in agreement with previous activity assays and site-specifically bound Mg^{2+} ions observed in the ribozyme's crystal structure (38, 39, 47, 48). The fraction of the most compact state increases gradually with increasing [Mg^{2+}] and reaches a maximum (10%) at 100 mM Mg^{2+}, with a $K_{Mg} = 25 \pm 2$ mM in the presence of PEG (10%) (Fig. 3*D*). In the absence of crowding agents, the most compact state appears only at concentrations above 20 mM Mg^{2+} (Fig. 3 *A*–*C*), with a midpoint of ribozyme folding of $K_{Mg} = 42 \pm 3$ mM (Fig. 3*D*), in agreement with previous results (31). These results show that the presence of PEG reduces the requirement of Mg^{2+} to reach the most compact state, N, the putative active state. The shift of the folding midpoint of the N state in the absence and presence of PEG by approximately twofold is in agreement with our activity assays (Fig. 1*C*), linking N-state formation with the ribozyme's activity.

Molecular Crowding Increases Dynamics Between Conformational States. From the smFRET time trajectories, it is possible to observe the different conformations adopted by the ribozyme in real time. As mentioned before, the N state (~0.6 FRET) is rarely populated and only transiently reached at high [Mg^{2+}]. In the absence of PEG and low [Mg^{2+}], three reoccurring FRET ratios (~0.1, ~0.21, and ~0.4) can be observed. The most compact state (~0.6 FRET) is absent. In contrast, the presence of 10% PEG 8000 at low [Mg^{2+}] accelerates the transitions between different conformations, and the N state becomes visible (Fig. 4*A*). Moreover, we distinguish between two types of FRET traces representing different states of activity: (*i*) dynamic molecules that show at least one transition between FRET states and (*ii*) static molecules that do not show any dynamics but have a constant FRET value. The overall number of dynamic molecules showing one or more transitions increases with increasing PEG percentage, reaching a maximum at 15%, and then decreases with higher PEG fractions (Fig. 4*B*). These results raise the interesting possibility that optimal PEG percentages enhance the formation of the most compact state by increasing its folding rate constant.

Molecular Crowding Agents Stabilize the Substrate-Bound Complex. To further understand the effect of crowding agents on the stability of the substrate-bound complex, we imaged single ribozyme molecules prebound to a 24-nt substrate comprising a cleavable (17/7) or noncleavable (17/7dC) 5′ splice site. The modified substrate has a deoxycytidine that slows cleavage 5 to 10 times relative to the wild type (49). In the absence of PEG, the fraction of the N state increases with substrate concentration (Fig. 5). At 30 mM Mg^{2+}, both substrates (17/7 and 17/7dC) bind the ribozyme with almost equal affinity ($K_{17/7} = 19 \pm 6$ nM and $K_{17/7dC}$ 20 ± 6 nM), suggesting that both substrates stabilize the ribozyme in similar magnitude. Previous studies have shown that the wild-type substrate binding increases the fraction of the compact state in comparison with the modified substrate at 100 mM Mg^{2+} (31). We observed a similar effect at 100 mM Mg^{2+} (*SI Appendix*, Fig. S5), but not at 30 mM Mg^{2+}, possibly because the ribozyme cannot fold correctly at low [Mg^{2+}]. To investigate the crowding effect on the substrate-bound complex, we performed experiments at various concentrations of both substrates in the presence of 10% PEG 8000 and 30 mM Mg^{2+}. Indeed, in the presence of PEG, the fraction of the most compact state increases with either substrate concentration (Fig. 5 *A* and *C*). Furthermore, substrate binding increases by a factor of ~2 for both 17/7 and 17/7dC ($K_{17/7} = 9 \pm 3$ nM and $K_{17/7dC} = 11 \pm 3$ nM; Fig. 5 *B* and *D*), indicating that molecular crowding favors the formation of the stable substrate-bound ribozyme complex, even at low [Mg^{2+}], which is consistent with the increase in the most compact state population by PEG 8000.

Discussion

How crowded cellular environments influence the activity of ribozymes has been a long-standing question (3). Recent studies have shown that crowding agents can affect both folding and catalytic rate constants of small and medium-sized ribozymes (13, 15, 17, 26–28, 30, 50, 51). However, how large ribozymes (relative to the crowder size) are affected has not been investigated until now. To address this question, we used the D135-L14 group II intron ribozyme construct as a model system to study the folding and catalysis of a large multidomain ribozyme

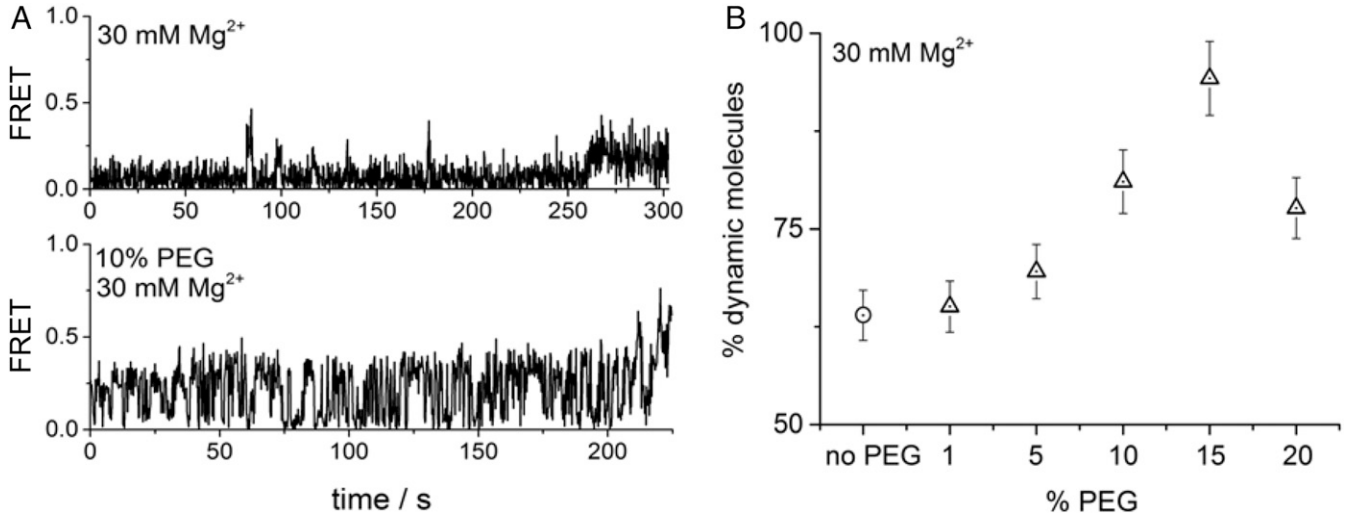

Fig. 4. Influence of a macromolecular crowded environment on ribozyme dynamics. (*A*) smFRET trajectories of D135-L14 show how the presence of PEG accelerates the ribozyme's conformational dynamics. (*B*) Fraction of dynamic molecules increases with PEG concentration. Error bars (SD) from triplicate experiments.

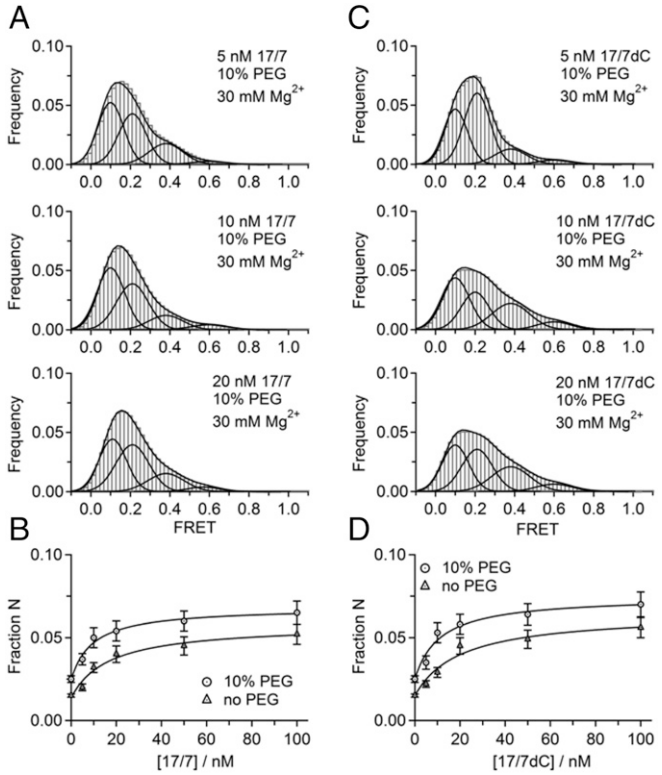

Fig. 5. Stabilizing effect of PEG on the ribozyme-substrate complex. (*A*) Effect of the increasing concentrations of the wild-type substrate (17/7) at 30 mM Mg^{2+} and 10% PEG 8000. (*B*) Fraction of the N state depending on the 17/7 concentration at 30 mM Mg^{2+} in the absence and presence of 10% PEG 8000. (*C*) Effect of different concentrations of the slow-cleavage substrate (17/7dC) at 30 mM Mg^{2+} and 10% PEG 8000. (*D*) Fraction of the N state at different concentrations of 17/7dC at 30 mM Mg^{2+} without and with 10% PEG 8000. Error bars (SD) determined via fitting of multiple Gaussians.

in crowded environments. Using PEG as a crowding agent that has negligible interactions with RNA (13,52), our ensemble-averaged cleavage assays show a fivefold increase in cleavage activity at low [Mg^{2+}] in the presence of PEG (10%) (Fig. 1), in agreement with previous studies with smaller ribozymes (13, 15, 17, 26–28, 30, 50, 51).

However, RNA molecules of different size and complexity can exhibit different responses to crowding agents (3). For example, low-molecular-weight crowders can destabilize small RNA constructs such as RNA hairpins (7) or the adenine riboswitch (53). For large ribozymes, it has been hypothesized, but never shown directly, that crowding effects may be different from those in small or medium-sized ribozymes (3, 54). In agreement with this hypothesis, our PEG titrations at near-physiological [Mg^{2+}] reveal optimum crowding conditions (10% PEG 8000) beyond which catalytic activity is hindered (Fig. 1*D*). A likely explanation for this observation is that, under optimum conditions, the interstitial space between crowding molecules defines an average cavity size that must match the size of the folded ribozyme (55). We note, however, that PEG is a diffusively dendritic polymer with an effective radius of gyration, but is not spherical in a physical sense. Therefore, overly dense conditions can decrease the ribozyme's activity. In agreement with this idea, the detrimental effect of "overcrowding" is attenuated with crowding agents of lower molecular weight (Fig. 1*D*).

To discriminate between effects in folding and catalysis, we used smFRET. The single-molecule data show that increasing PEG concentrations result in both a higher population of the most compact state (N) and a decrease in Mg^{2+} ion requirements for folding (Figs. 2 and 3). These findings are in line with previous results showing that crowding agents favor folded compact conformations (13–15, 27, 28, 54). Interestingly, we did not observe an optimal PEG concentration for folding as in the activity assay (compare Figs. 1*D* and 2*D*). A possible explanation of this apparent discrepancy may be that once the various ribozyme's folding intermediates reach a minimum radius of gyration, they no longer benefit from additional crowding-induced stabilization (28), thereby explaining the observed saturation in the PEG titration.

An additional interesting observation from the single-molecule trajectories is that crowding agents not only stabilize the most compact state but also increase their dynamics (Fig. 4). This result implies that crowded environments can accelerate folding rate constants by stabilizing folding transition states, as observed for the hairpin ribozyme (13), an effect similar to that of RNA helicases (34).

We also observed that crowding agents stabilize the ribozyme–substrate complex equally for cleavable and noncleavable substrates (Fig. 5), raising the interesting possibility that molecular crowding helps to partially curb the effect of mutations on folding and catalysis. A similar effect was recently observed for the group I intron ribozyme, whereby crowders helped to partially offset tertiary contact mutations that reduce activity under physiological conditions (29).

In summary, the combination of activity assays and single-molecule studies shows that excluded volume effects can play important roles in both folding and catalysis of large ribozymes, such as the D135-L14 ribozyme, by stabilizing the most compact (i.e., native) conformation and transition states between folding intermediates. However, beyond an optimal crowding concentration, activity can be hindered by stabilization of compact but inactive folding intermediates. Therefore, whether the crowded environment inside cells and organelles, such as mitochondria where group II introns are expressed (56), affects the folding and activity of large catalytic RNAs will need to be investigated directly. To the best of our knowledge, cavity sizes have never been directly measured in eukaryotic cells. Therefore, we cannot compare the distribution of polymer sizes with cavity sizes in the cell. However, given that the cell is made of heterogenous crowding agents, we can reasonably speculate that the cell provides a broad, heterogeneous distribution of cavity sizes. Furthermore, this distribution is likely to be dynamic and to adapt, for example, as the cell moves and as its contents change with the cell cycle. It is possible, therefore, that cavity sizes in cells adjust as RNA and protein molecules fold into their most compact state (often the N state).

Methods

RNA Preparation and Cleavage Activity Assays. The D135-L14 ribozyme was obtained from the transcription of the plasmid pT7D135-L14, derived from the plasmid pT7D135 carrying the sequence coding for the *S. cerevisiae* intron ai5γ modified with the insertion of two loops and the overhang at the 3′ via mutational PCR. Upon HindIII digestion, the linearized pT7D135-L14 was transcribed with homemade T7 polymerase, purified via denaturing gel eletrophoresis, extracted by crush-and-soak, and stored at −20 °C in water (57). The reaction was performed under single turnover conditions using ^{32}P-labeled substrate at standard conditions (80 mM 3-(N-morpholino)propanesulfonic acid, pH 6.9; 500 mM KCl) at 42 °C and varying [Mg^{2+}] (33). The desired percentage of PEG was dissolved in the solutions containing ribozyme and/or substrate (*SI Appendix, SI Methods*).

Single-Molecule Experiments. smFRET experiments were conducted by hybridizing Cy3, Cy5, and biotin-labeled DNA to the two loops and the 3′ elongation of the ribozyme, respectively (31, 32, 58, 59). Next, the solution containing the labeled ribozyme was diluted to 50 to 100 pM for surface immobilization on a BSA-passivated surface. To form the substrate-bound complex, the substrate was preincubated in the microfluidic channel with preimmobilized ribozyme. PEG solutions at desired [Mg^{2+}] were prepared in imaging buffer by mixing with an oxygen scavenging system and were injected into the microfluidic channel before imaging. The donor fluorophores

were excited using a 532 nm laser at the total internal reflection angle, and emission signals from both donor and acceptor fluorophores were collected using a water immersion objective (60×). Next, signals were filtered and separated using dual-view and then imaged on two halves of a high quantum yield EM-CCD camera chip (Andor). Single-molecule videos were analyzed as described previously (31, 32, 58, 60).

ACKNOWLEDGMENTS. E.F. thanks Mélodie C. A. S. Hadzic, Sebastian L. B. König, and Danny Kowerko for their support regarding the smFRET setup and software development, as well as Susann Zelger-Paulus for helpful discussions regarding the group II intron ribozyme. This work was supported by a core grant of the Medical Research Council London Institute of Medical Sciences (UKRI MC-A658-5TY10) (to D.S.R.), Imperial College London start-up funds (D.S.R.), the European Research Council Starting Grant MIRNA 259092 (to R.K.O.S.), and University of Zurich Forschungskredit Grants FK-14-096 and FK-15-095 (to R.B.). R.K.O.S. thanks the Swiss National Science Foundation and the Swiss State Secretariat for Education and Research (COST Action CM1105) for further financial support related to our smFRET studies.

1. Ellis RJ (2001) Macromolecular crowding: Obvious but underappreciated. *Trends Biochem Sci* 26:597–604.
2. Miyoshi D, Sugimoto N (2008) Molecular crowding effects on structure and stability of DNA. *Biochimie* 90:1040–1051.
3. Nakano S, Miyoshi D, Sugimoto N (2014) Effects of molecular crowding on the structures, interactions, and functions of nucleic acids. *Chem Rev* 114:2733–2758.
4. Politou A, Temussi PA (2015) Revisiting a dogma: The effect of volume exclusion in molecular crowding. *Curr Opin Struct Biol* 30:1–6.
5. Zhou HX, Rivas G, Minton AP (2008) Macromolecular crowding and confinement: Biochemical, biophysical, and potential physiological consequences. *Annu Rev Biophys* 37:375–397.
6. Minton AP (2001) The influence of macromolecular crowding and macromolecular confinement on biochemical reactions in physiological media. *J Biol Chem* 276: 10577–10580.
7. Gao M, et al. (2016) RNA hairpin folding in the crowded cell. *Angew Chem Int Ed Engl* 55:3224–3228.
8. Zhou HX (2013) Influence of crowded cellular environments on protein folding, binding, and oligomerization: Biological consequences and potentials of atomistic modeling. *FEBS Lett* 587:1053–1061.
9. Russell R, ed (2013) *Biophysics of RNA Folding* (Springer, New York).
10. Marcia M, Pyle AM (2014) Principles of ion recognition in RNA: Insights from the group II intron structures. *RNA* 20:516–527.
11. Bowman JC, Lenz TK, Hud NV, Williams LD (2012) Cations in charge: Magnesium ions in RNA folding and catalysis. *Curr Opin Struct Biol* 22:262–272.
12. Sigel A, Sigel H, eds (2011) *Structural and Catalytic Roles of Metal Ions in RNA* (R Soc Chem, Cambridge, UK).
13. Paudel BP, Rueda D (2014) Molecular crowding accelerates ribozyme docking and catalysis. *J Am Chem Soc* 136:16700–16703.
14. Dupuis NF, Holmstrom ED, Nesbitt DJ (2014) Molecular-crowding effects on single-molecule RNA folding/unfolding thermodynamics and kinetics. *Proc Natl Acad Sci USA* 111:8464–8469.
15. Kilburn D, Roh JH, Guo L, Briber RM, Woodson SA (2010) Molecular crowding stabilizes folded RNA structure by the excluded volume effect. *J Am Chem Soc* 132: 8690–8696.
16. Denesyuk NA, Thirumalai D (2011) Crowding promotes the switch from hairpin to pseudoknot conformation in human telomerase RNA. *J Am Chem Soc* 133: 11858–11861.
17. Nakano S, Kitagawa Y, Yamashita H, Miyoshi D, Sugimoto N (2015) Effects of co-solvents on the folding and catalytic activities of the hammerhead ribozyme. *ChemBioChem* 16:1803–1810.
18. Choi SI, et al. (2013) Protein folding in vivo revisited. *Curr Protein Pept Sci* 14:721–733.
19. Zhou HX (2013) Polymer crowders and protein crowders act similarly on protein folding stability. *FEBS Lett* 587:394–397.
20. Samiotakis A, Wittung-Stafshede P, Cheung MS (2009) Folding, stability and shape of proteins in crowded environments: Experimental and computational approaches. *Int J Mol Sci* 10:572–588.
21. Ladurner AG, Fersht AR (1999) Upper limit of the time scale for diffusion and chain collapse in chymotrypsin inhibitor 2. *Nat Struct Biol* 6:28–31.
22. Jacob M, Schindler T, Balbach J, Schmid FX (1997) Diffusion control in an elementary protein folding reaction. *Proc Natl Acad Sci USA* 94:5622–5627.
23. Ebbinghaus S, Dhar A, McDonald JD, Gruebele M (2010) Protein folding stability and dynamics imaged in a living cell. *Nat Methods* 7:319–323.
24. Cheung MS, Klimov D, Thirumalai D (2005) Molecular crowding enhances native state stability and refolding rates of globular proteins. *Proc Natl Acad Sci USA* 102: 4753–4758.
25. Heddi B, Phan AT (2011) Structure of human telomeric DNA in crowded solution. *J Am Chem Soc* 133:9824–9833.
26. Desai R, Kilburn D, Lee HT, Woodson SA (2014) Increased ribozyme activity in crowded solutions. *J Biol Chem* 289:2972–2977.
27. Strulson CA, Yennawar NH, Rambo RP, Bevilacqua PC (2013) Molecular crowding favors reactivity of a human ribozyme under physiological ionic conditions. *Biochemistry* 52:8187–8197.
28. Kilburn D, Roh JH, Behrouzi R, Briber RM, Woodson SA (2013) Crowders perturb the entropy of RNA energy landscapes to favor folding. *J Am Chem Soc* 135:10055–10063.
29. Lee HT, Kilburn D, Behrouzi R, Briber RM, Woodson SA (2015) Molecular crowding overcomes the destabilizing effects of mutations in a bacterial ribozyme. *Nucleic Acids Res* 43:1170–1176.
30. Nakano S, Karimata HT, Kitagawa Y, Sugimoto N (2009) Facilitation of RNA enzyme activity in the molecular crowding media of cosolutes. *J Am Chem Soc* 131: 16881–16888.
31. Steiner M, Karunatilaka KS, Sigel RKO, Rueda D (2008) Single-molecule studies of group II intron ribozymes. *Proc Natl Acad Sci USA* 105:13853–13858.
32. Steiner M, Rueda D, Sigel RKO (2009) Ca2+ induces the formation of two distinct subpopulations of group II intron molecules. *Angew Chem Int Ed Engl* 48:9739–9742.
33. Swisher JF, Su LJ, Brenowitz M, Anderson VE, Pyle AM (2002) Productive folding to the native state by a group II intron ribozyme. *J Mol Biol* 315:297–310.
34. Karunatilaka KS, Solem A, Pyle AM, Rueda D (2010) Single-molecule analysis of Mss116-mediated group II intron folding. *Nature* 467:935–939.
35. Fedorova O, Zingler N (2007) Group II introns: Structure, folding and splicing mechanism. *Biol Chem* 388:665–678.
36. Lambowitz AM, Zimmerly S (2011) Group II introns: Mobile ribozymes that invade DNA. *Cold Spring Harb Perspect Biol* 3:a003616.
37. Toor N, Keating KS, Pyle AM (2009) Structural insights into RNA splicing. *Curr Opin Struct Biol* 19:260–266.
38. Robart AR, Chan RT, Peters JK, Rajashankar KR, Toor N (2014) Crystal structure of a eukaryotic group II intron lariat. *Nature* 514:193–197.
39. Chan RT, Robart AR, Rajashankar KR, Pyle AM, Toor N (2012) Crystal structure of a group II intron in the pre-catalytic state. *Nat Struct Mol Biol* 19:555–557.
40. Galej WP, et al. (2016) Cryo-EM structure of the spliceosome immediately after branching. *Nature* 537:197–201.
41. Su LJ, Waldsich C, Pyle AM (2005) An obligate intermediate along the slow folding pathway of a group II intron ribozyme. *Nucleic Acids Res* 33:6674–6687.
42. Fiorini E, Börner R, Sigel RKO (2015) Mimicking the in vivo environment–The effect of crowding on RNA and biomacromolecular folding and activity. *Chimia (Aarau)* 69: 207–212.
43. Gonzalez-Tello P, Camacho F, Blazquez G (1994) Density and viscosity of concentrated aqueous solutions of polyethylene glycol. *J Chem Eng Data* 39:611–614.
44. Kapanidis AN, et al. (2004) Fluorescence-aided molecule sorting: Analysis of structure and interactions by alternating-laser excitation of single molecules. *Proc Natl Acad Sci USA* 101:8936–8941.
45. Pincus DL, Hyeon C, Thirumalai D (2008) Effects of trimethylamine N-oxide (TMAO) and crowding agents on the stability of RNA hairpins. *J Am Chem Soc* 130:7364–7372.
46. Michel F, Ferat JL (1995) Structure and activities of group II introns. *Annu Rev Biochem* 64:435–461.
47. Pyle AM (2010) The tertiary structure of group II introns: Implications for biological function and evolution. *Crit Rev Biochem Mol Biol* 45:215–232.
48. Sigel RKO, Vaidya A, Pyle AM (2000) Metal ion binding sites in a group II intron core. *Nat Struct Biol* 7:1111–1116.
49. Griffin EA, Jr, Qin Z, Michels WJ, Jr, Pyle AM (1995) Group II intron ribozymes that cleave DNA and RNA linkages with similar efficiency, and lack contacts with substrate 2′-hydroxyl groups. *Chem Biol* 2:761–770.
50. Hervé G, Tobé S, Heams T, Vergne J, Maurel MC (2006) Hydrostatic and osmotic pressure study of the hairpin ribozyme. *Biochim Biophys Acta* 1764:573–577.
51. Giel-Pietraszuk M, Barciszewski J (2012) Hydrostatic and osmotic pressure study of the RNA hydration. *Mol Biol Rep* 39:6309–6318.
52. Lambert D, Draper DE (2007) Effects of osmolytes on RNA secondary and tertiary structure stabilities and RNA-Mg2+ interactions. *J Mol Biol* 370:993–1005.
53. Tyrrell J, Weeks KM, Pielak GJ (2015) Challenge of mimicking the influences of the cellular environment on RNA structure by PEG-induced macromolecular crowding. *Biochemistry* 54:6447–6453.
54. Nakano S, Kitagawa Y, Miyoshi D, Sugimoto N (2014) Hammerhead ribozyme activity and oligonucleotide duplex stability in mixed solutions of water and organic compounds. *FEBS Open Bio* 4:643–650.
55. Kang H, Pincus PA, Hyeon C, Thirumalai D (2015) Effects of macromolecular crowding on the collapse of biopolymers. *Phys Rev Lett* 114:068303.
56. Rudan M, et al. (2018) Normal mitochondrial function in *Saccharomyces cerevisiae* has become dependent on inefficient splicing. *eLife* 7:e35330.
57. Gallo S, Furler M, Sigel RKO (2005) In vitro transcription and purification of RNAs of different size. *Chimia (Aarau)* 59:812–816.
58. Zhao R, Rueda D (2009) RNA folding dynamics by single-molecule fluorescence resonance energy transfer. *Methods* 49:112–117.
59. Cardo L, Karunatilaka KS, Rueda D, Sigel RKO (2012) Single molecule FRET characterization of large ribozyme folding. *Methods Mol Biol* 848:227–251.
60. Börner R, Kowerko D, Miserachs HG, Schaffer MF, Sigel RKO (2016) Metal ion induced heterogeneity in RNA folding studied by smFRET. *Coord Chem Rev* 327-328:123–142.